Upgrade of Thermal Compensation System for Enhanced LIGO

Darcy Barron

Mentors: Phil Willems, Rana Adhikari, Tobin Fricke

Abstract

The LIGO thermal compensation system corrects thermal distortions in the optics caused by heating from the main laser beam. A CO_2 laser remotely heats the entire optic in a central or annular heating pattern. The planned upgrade of the LIGO interferometers from Initial LIGO to Enhanced LIGO will include increasing the laser power of the main beam. The increased power will require greater thermal compensation power. A new laser optical table has been set up and the power of the thermal compensation system is being upgraded from 10 W to 35 W. This power upgrade requires intensity stabilization of the laser to reduce noise coupling to the interferometer. Also, the annular mask currently used to create the annular heating pattern will be replaced by conical optics.

Introduction/Background

The LIGO project is attempting to detect gravitational waves, which are waves in space-time predicted by general relativity. The systems used by LIGO to detect gravitational waves are Michelson interferometers, with long arms and resonating Fabry-Perot cavities to maximize length. Laser light goes through a beam splitter and down two perpendicular arms, and then returns to the beam splitter. If the arms are the same length, or if the length differs by an integral number of wavelengths, the light beams will interfere destructively, resulting in no light being detected at the asymmetric port. A gravitational wave would cause a decrease in length along one direction and an increase in length along an orthogonal direction, which would result in the arms having slightly different lengths. This difference in length would cause a difference in the phase of the light beams, and the beams would not completely cancel each other out, leaving light that is read as the gravitational wave signal.[1]

To be able to detect gravitational waves, the sensitivity of the interferometer must be greater than about 10^{-19} m/√Hz. At very low frequencies, thermal, seismic, and quantum sources of noise limit the sensitivity. The peak sensitivity of the LIGO interferometers is at about 100 Hz. A graph of the sensitivity of initial LIGO along with the limits of sensitivity is shown in Figure 1.[2]

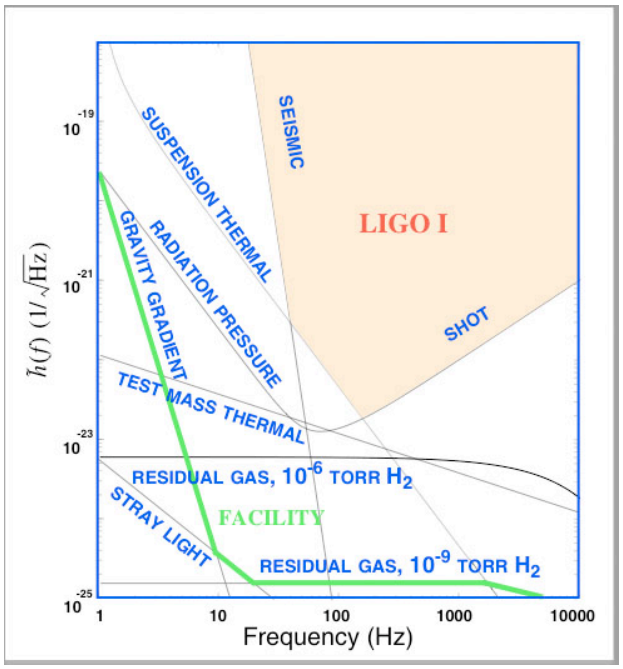

Figure 1. Sensitivity of Initial LIGO and noise sensitivity limits

The arms of the interferometer have additional input mirrors to create Fabry-Perot cavities, which increases the effective length of the arm and the storage time of light. The arms are locked using the Pound-Drever-Hall locking scheme. The current Initial LIGO laser is a 10 W Nd:YAG laser, with an optical input of 6 W to the interferometer. There are 3 pairs of RF sidebands along with the main carrier beam. The main beam resonates in all cavities, but the sidebands resonate only in some of the cavities, and not the arms. Sidebands created by a gravitational wave in the arms are heterodyned against an RF sideband to create the gravitational wave signal.[3]

The LIGO detectors are currently in their initial stage, and have completed several science runs and have reached design sensitivity. Starting in 2007, many improvements and upgrades will be made to the design to improve the sensitivity of the detectors, and this new phase will be called Enhanced LIGO. The laser input power will increase from 7 W in Initial LIGO to 35 W for Enhanced LIGO, which will cause the power circulating in the cavities to increase from 15 kW to 36 kW. Because of the high power of the laser, thermal distortions are created. If this is not compensated for, the detector will not function properly. The main thermal effects that modify the optics are thermoelastic deformation and thermal lensing. These create wavefront distortions that decrease the gravitational wave strain sensitivity of the instrument by decreasing the arm cavity gain for the carrier, decreasing the power recycling cavity gain for the carrier and the sidebands, and increasing the total carrier power leaking out of the dark port.[4] The increase in main laser power requires an increase in the power of the thermal compensation system laser because the mirrors require more thermal compensation.

This summer, a new laser optical table was set up to prepare for the future upgrade of the thermal compensation system from 10 W to 35 W. The project included working on intensity stabilization of the carbon dioxide laser. This is necessary because noise in the thermal compensation can couple to output noise of the interferometer. First, I will discuss the current implementation of the thermal compensation and the plans for the upgrade. The next section will discuss the intensity stabilization of the laser, including the stabilization servo. Finally, I will discuss the future work that will be done on the project.

Thermal Compensation System Design

The LIGO optics were designed to operate with a certain amount of thermal lensing, based on the estimated absorption of the mirrors and a laser power of about 6 W. The absorption of the mirrors was expected to be about 1 ppm from the HR coating and 10 ppm/cm from the substrate.[5] However, the absorption of the mirrors is more than expected, and the laser power has been less than 6 W for Initial LIGO, and will be increased greatly for Enhanced LIGO. The absorptions for the optics used in the LIGO interferometers are shown in Table 1.

	H1	H2[6]	L1[7]
ITMX	NA	-1.9 ± 3.7 ppm	2.3 ± 0.9 ppm
ITMY	NA	11.6 ± 2.3 ppm	6.6 ± 1.5 ppm
ETMX	NA	3.8 ± 3.5 ppm	NA
ETMY	NA	5.7 ± 1.1 ppm	NA

Table 1. Absorption of optics in LIGO interferometers.

The mirrors will need corrective heating in either a central shape or an annular shape, depending on the level of heating of the mirror from the main laser. The current required heating shape for each optic is shown in Table 2.

	H1[8]	H2[9]	L1[10]
ITMX	Central	None	Annular
ITMY	Central	Annular	Central

Table 2. Required heating for LIGO optics.

The thermal compensation projector is used to remotely heat the optic using a CO_2 laser. The layout of the thermal compensation system optical bench is shown in Figure 2. The beam passes through the beam shaping optical system and the heating pattern is projected onto the mirror using a projection telescope.

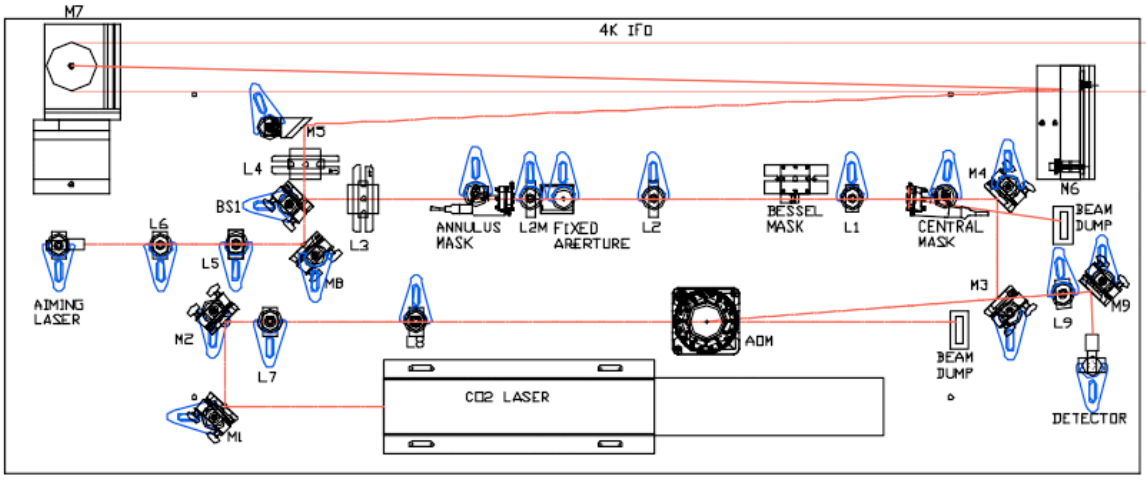

Figure 2. Layout of thermal compensation system.

The projector can heat in a central heating mode or an annular heating mode. The central heating mode produces a Gaussian central heating spot. The beam passes through a mask with a central hole with the desired diameter. The annular mode is also a Gaussian profile, but it has a certain diameter hole where there is no beam in the center. An annular mask is currently being used to achieve this annular heating pattern.

Intensity Stabilization

The first step of the project is working on intensity stabilization of the carbon dioxide laser. The relative intensity noise (RIN) of the 10 W system was about 2×10^{-6} $1/\sqrt{\text{Hz}}$ in the relevant bandwidth of 40 - 500 Hz.[11]

The expected effect of intensity noise on displacement noise in the interferometer for central heating mode is given by

$$< \Delta z >= 10^{-20} \frac{m}{\sqrt{Hz}} \left(\frac{150Hz}{f} \right) \left(\frac{P}{25mW} \right) \left(\frac{RIN}{4 \times 10^{-6} Hz^{-1/2}} \right)$$

For annular heating, it is given by[12]

$$< \Delta z >= 1.4 \times 10^{-17} m \left(\frac{150Hz}{f} \right) \left(\frac{P}{1mWatt} \right) RIN$$

where RIN is the relative intensity noise of the laser, P is the power absorbed in the substrates, and f is the modulation frequency.[13] For 12 kW of power circulating in the cavity and an absorption of 5 ppm, the power will be 60 mW, and for annular heating there is a factor of 11:1 increase, so the power will be 660 mW. For the RIN of the

stabilized and unstabilized laser, I used the photodiode RIN for the stabilized laser and the open loop RIN for the unstabilized laser. These noise contributions are compared with the Initial LIGO and expected Enhanced LIGO sensitivity curves in Figure 3.

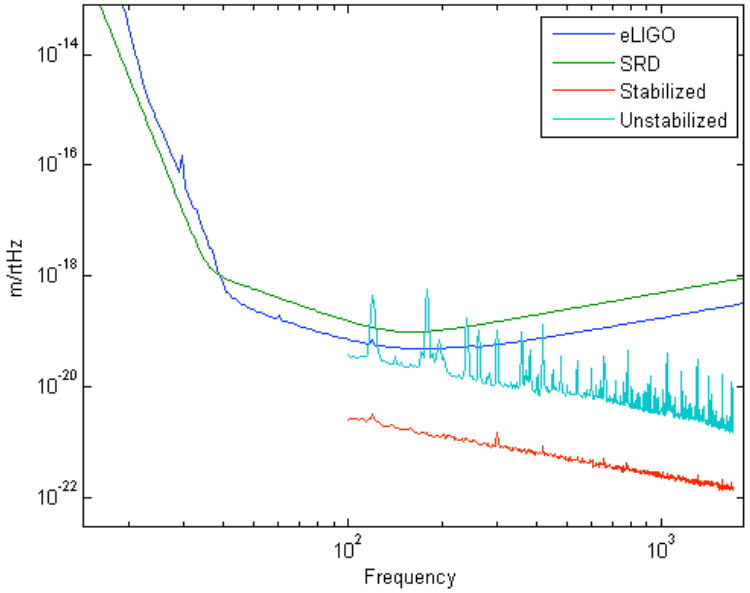

Figure 3. Noise contribution of stabilized and unstabilized TCS laser.

An intensity stabilization servo for the upgraded system has been designed and set up, and is shown in Figure 4.[14]

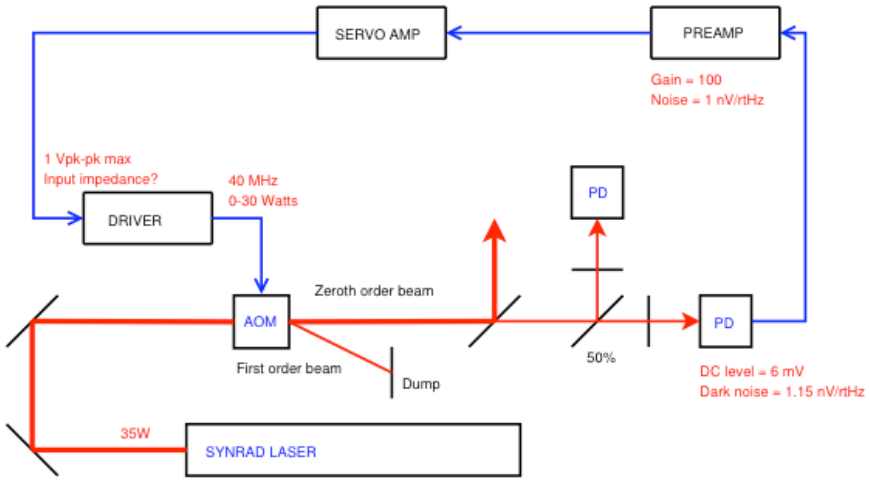

Figure 4. Design of intensity stabilization servo.

The beam from the 35 W CO2 laser goes through an acousto-optic modulator (AOM) and then goes through two mirrors where a small amount of light is directed to

two photodiodes. The remaining light goes into a power meter. The AOM is used to modulate the intensity of the light by controlling how much of the beam is deflected by the acousto-optic effect. The first photodiode measures the intensity of the light it receives, which is sent through a low-noise preamplifier, and then fed into the servo and back into the AOM to stabilize fluctuations in intensity. The second photodiode is located out of the feedback loop to independently measure the intensity fluctuations. A photo of the optical table, configured for a photodiode measurement, is shown in Figure 5.

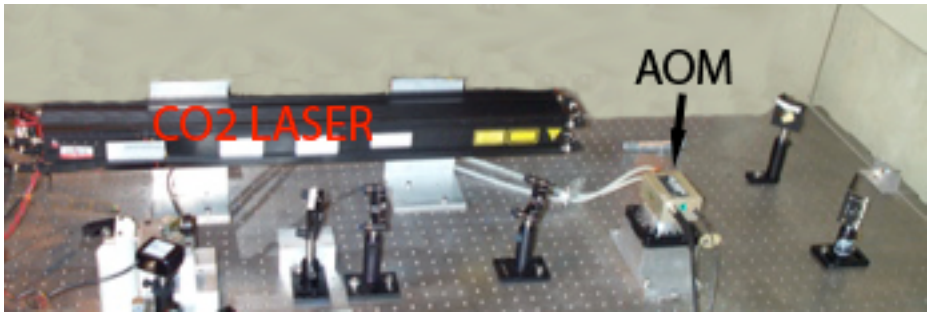

Figure 5. Photo of CO2 laser and AOM in setup for photodiode measurement.

Several low-noise preamplifiers were tested to determine their noise spectra (see Methods part 1). A comparison of the input-referred noise for three preamplifiers is shown in Figure 6.

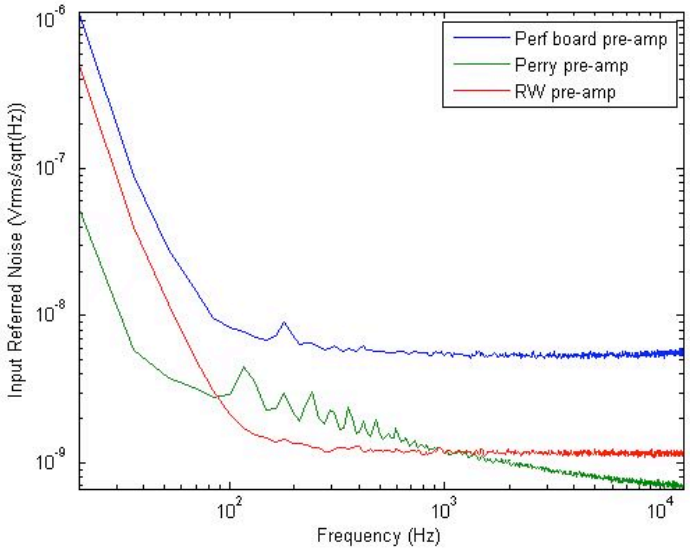

Figure 6. Input-referred noise spectra of preamplifiers.

The preamplifier with the lowest noise was designed to be powered by batteries, but for a permanent solution the preamplifier will need to be powered by a power supply. A comparison of the preamplifier running off batteries and off a power supply, shown in Figure 7, show that the noise spectra are very similar.

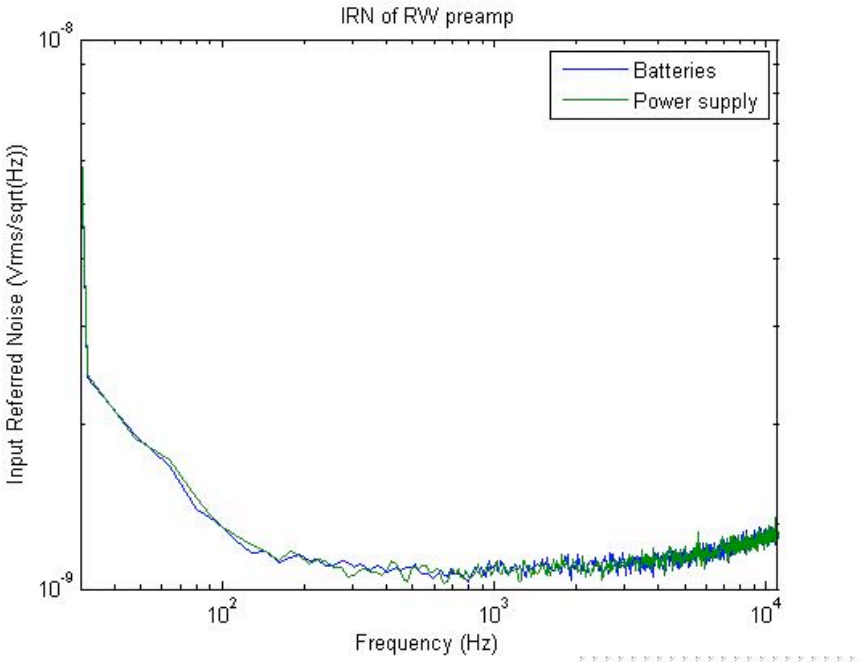

Figure 7. Input referred noise for preamplifier powered by batteries and a power supply.

The board design of the low-noise, battery-powered preamplifier was redesigned for the preamplifier to run off a power supply. The new boards were ordered, and one of the preamplifiers was partially assembled. However, the noise was much higher than the expected design value of 0.4 nV/√Hz, and various components including thin-film resistors will be tested to reduce the noise.

To measure the intensity noise of the laser, photodiodes will be used, so an accurate measurement of their noise level needs to be determined. Movement of the position of the beam may cause noise to appear at the photodiode. New photodiode mounts were made this summer to further stabilize them. The structure of the photodiode is unknown, but it must be determined so that its spatial response can be determined. The photodiode may be composed of layers of photosensitive materials, with unresponsive layers in between.[15] If this is the case, movement of a beam that is filling only part of the photodiode will cause noise. To study the structure of the photodiode, it was first

examined under a microscope. The surface showed no signs of a pattern or structure. A photo of one of the photodiodes is shown in Figure 8.

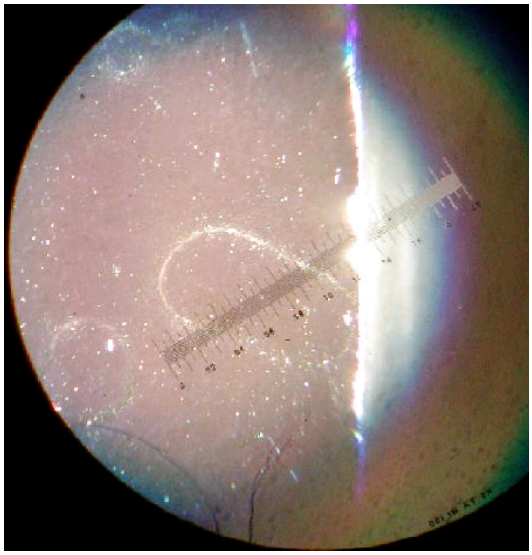

Figure 8. Photo of photodiode under a microscope.

Next, an optical arrangement was set up to put a very small, low-intensity beam on the photodiode to scan its surface (See Methods part 2). The beam was reduced to a beam waist radius of 0.11 mm and an intensity of less than 0.02 W. The photodiode was mounted on a translational stage to scan the surface. The results of two horizontal scans across the middle of the photodiode are shown in Figure 9.

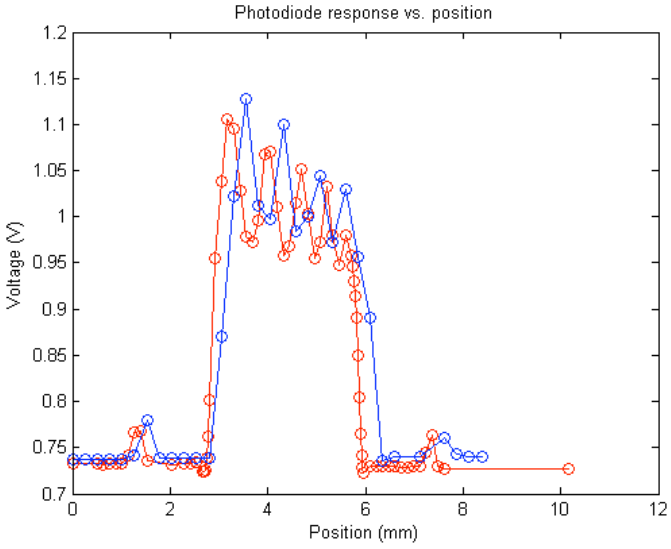

Figure 9. Photodiode response vs. position for two scans.

The results of two vertical scans across the middle of the photodiode are shown in Figure 10.

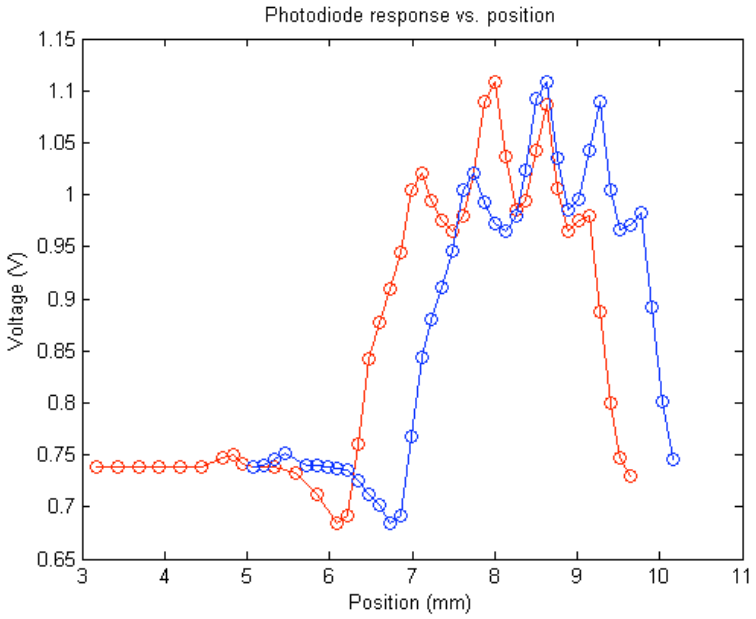

Figure 10. Photodiode response vs. position for two scans.

The difference in position between the two scans can be attributed to small shifts in the setup as it was moved back and forth. The overall pattern, however, remains the same between both scans. The pattern is similar to a diffraction pattern, and it must be investigated if that is the cause of the inhomogeneous response.

Another method to measure the spatial response was using a pinhole very close to the photodiode to reduce the beam size. However, our attempts at this method proved unsuccessful (see Methods part 3).

An automated photodiode scanning setup is being constructed so that the photodiode can be scanned many times and a map of the response over its entire surface can be made (see Methods part 4). The automated scanner is not yet completed.

Future Work

The thermal compensation system upgrade was not yet completed at the end of the summer. Once the automated scanner is completed, it should be able to provide a detailed 2-D map of the diode surface. If there are significant inhomogeneities in the

spatial response, this will need to be combined with the expected beam motion to get an estimated noise contribution. The laser will also need a more stable mount to reduce movement of the beam. Also, new axicon lenses will be used to create the annular heating mode, replacing the annular mask. Once the laser has been stabilized to an acceptable level and other portions of the project are complete, the upgraded system will be ready to install at the sites. The installation will start once the current data run is completed in early 2008.

Methods Appendix

1. Preamplifier noise measurements

To measure the input referred noise of a preamplifier, the preamplifier's output was connected to the channel of a spectrum analyzer, and the input was terminated with a 50-ohm resistor. The resulting spectrum was divided by the expected gain of the preamplifier to get the input referred noise. The Perry preamplifier had a gain of 1397, and the preamplifiers based on the design by Rai Weiss had an expected gain of 100.

To compare the noise spectra with the preamplifier running off power supply and battery, the battery preamplifier was connected with clips to a power supply and the noise spectra was taken again. To measure the powered preamplifier running off of a battery, battery clips were connected to a battery and then connected to the preamplifier after the voltage regulators.

2. Measuring spatial response of photodiodes with lens setup

The beam size was reduced with a lens with a focal length F of 3 inches, with the photodiode placed at the focal point. For an incident beam with a wavelength λ of 10.64 μm and a diameter D of 4.6 mm, this will create a beam waist radius ω_o of 0.11 mm.

$$\theta = \frac{4\lambda}{2\pi\omega_0}$$

$$\theta \approx \frac{D}{F}$$

$$\omega_0 \approx \frac{2\lambda}{\pi}\frac{F}{D}$$

The photodiodes are only capable of receiving 100 W/cm^2, so the intensity of this beam must be low enough to not damage the photodiode. For a Gaussian beam, the average intensity is one-half of the peak intensity of the beam. Therefore, a 0.11 mm beam will need a power of less than 0.02 W in order to not damage the photodiode.

The main laser controller controlled the power of the laser by changing the duty cycle of the laser pulses. This would introduce noise into the measurement, so the power of the laser was set to its maximum (constant pulse) and highly reflective mirrors were used to dump excess light. The mirrors were tested to verify their reflectivity, and also tested to determined their reflectivity at different angles. The maximum reflectivity was when the incident light was nearly normal, so this was how they were placed in the setup, shown in Figure 11.

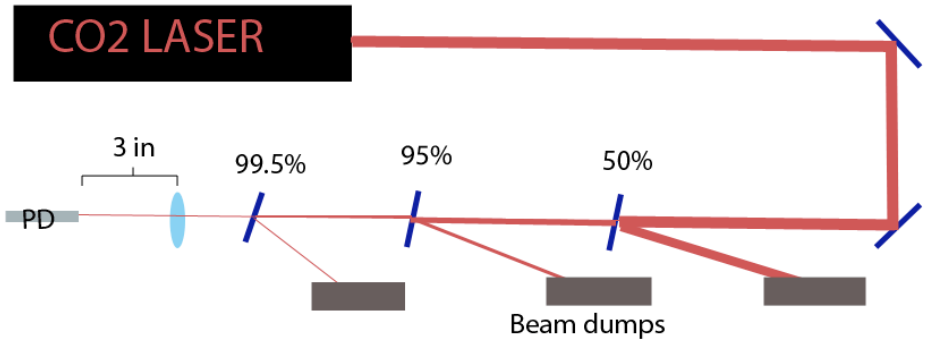

Figure 11. Setup for measurement of photodiode response.

The laser was 10.64 mm invisible radiation that was detected using cards with ultraviolet light also shining on them. The material would fluoresce, but not in the spot where the beam was, so the beam was detectable as a dark spot. Working with such low powers for the photodiode measurement meant that the beam was impossible to detect after the final mirror. To align the setup so that the beam was on the photodiode, first a thin beam dump was placed in front of the photodiode to protect it. IR-sensitive paper was placed on the beam dump with a "crosshairs" drawn on it that was aligned with the

center of the photodiode. Because the lens had a short 3-inch focal length, a steering mirror couldn't be placed between the lens and the photodiode, so the position of the photodiode had to be adjusted instead. With the first two mirrors in place (beam splitter 50% reflective mirror and 95% reflective mirror), the photodiode was adjusted to the correct position by observing the darkened spots on the IR paper. Also, the brick beam dumps were carefully positioned to absorb all reflected light from the mirrors. Next, the 99.5% reflective mirror was added to the optical path, and its reflection properly dumped. Finally, the beam dump blocking the photodiode was removed.

The photodiode was mounted on a calibrated translational stage. The photodiode was moved around slowly until a signal was observed (using either an oscilloscope or a voltmeter connected to the photodiode). After the positions of the edges of the photodiode were established, data could be taken.

3. Measuring spatial response of photodiode using pinholes

Instead of using a lens to reduce the beam size, another possibility is passing the beam through a very small pinhole. Pinholes that were 50 and 100 microns in size were made in a small metal sheet. The pinholes had to be placed very near to the photodiode to reduce diffraction effects. This method required that the pinhole move as the beam and photodiode remain in the same position. However, the metal sheet that the pinholes were in was reflective at the laser's wavelength, and the incident radiation had to be kept relatively small to prevent damage, and this also meant moving the pinhole was difficult. Possible changes to make this method work would be to make the pinhole in a different, less reflective material and to make jagged pinholes to reduce diffraction effects.

4. Automated photodiode scanner

For an automated scan, instead of changing the position of the photodiode, galvanometers will be used to move two mirrors to change the position of the beam. The galvanometers will move the mirror by a certain angle for a certain amount of current supplied. The calibration curve is shown in Figure 12.

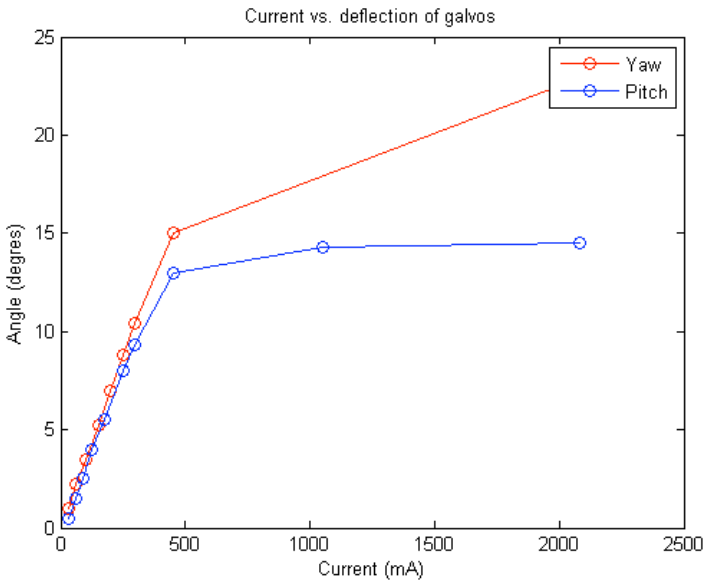

Figure 12. Current vs. angle for galvanometer.

The current will be supplied by a computer data acquisition system, which can only output a small amount of current. Therefore, current amplifiers will be necessary to obtain the required range to scan the entire photodiode.

An old photodiode scanner was reassembled and repositioned to make the automated setup. Since the focal length of the lens was only 3 inches, the scanning mirrors had to be placed very close together so that the photodiode was located at the focal point. The closest mirror would be 1 inch away from the photodiode, and would need to scan over a distance of 2 mm for the largest photodiode. This requires an angle of 45 degrees, and therefore a current of 150 mA. The computer data acquisition system can only output a current of 10 mA, so a current amplifier with a gain of 25 was built.

References

[1] Black, Eric D. and Ryan N. Gutenkunst. "An introduction to signal extraction in interferometric gravitational wave detectors." Am. J. Phys. 71.4 (2003). 365-378

[2] Weiss, Rainer. "Sensitivity Improvement and Gravitational Wave Detection." NSF Advanced LIGO Review. http://www.ligo.caltech.edu/NSF/related/05.2006/plenaries-weiss.pdf

[3] Willems, Phil. "Nonlinear Optical Effects in the LIGO Gravitational-wave Interferometer." LIGO Technical Report. http://www.ligo.org/pdf_public/willems.pdf

[4] Lawrence, Ryan Christopher. "Active Wavefront Correction in Laser Interferometric Gravitational Wave Detectors." Doctoral thesis, February 2003, Massachusetts Institute of Technology.

[5] Ballmer, Stefan W. "LIGO interferometer operating at design sensitivity with application to gravitational radiometry." Doctoral thesis, June 2006, Massachusetts Institute of Technology.

[6] http://ilog.ligo-wa.caltech.edu/ilog/pub/ilog.cgi?group=detector&task=view&date_to_view=02/26/2007&anchor_to_scroll_to=2007:02:26:12:38:27-willems

[7] http://ilog.ligo-wa.caltech.edu:7285/mLIGO/TCS/LLO

[8] http://www.ligo-wa.caltech.edu/

[9] http://www.ligo-wa.caltech.edu/

[10] http://london.ligo-la.caltech.edu/

[11] Ballmer, thesis.

[12] Ballmer, thesis.

[13] Ballmer et al. "Thermal Compensation System Description." LIGO-T050064-00-R

[14] http://ilog.ligo-wa.caltech.edu:7285/mLIGO/TCS/CO2_Stabilization?action=AttachFile&do=get&target=co2servo.pdf

[15] Discussion with Phil Willems

Acknowledgements

Thanks to Tobin Fricke, Rana Adhikari, Phil Willems, Alan Weinstein, Ken Libbrecht, and everyone at 40-meter lab and Wilson House for their help, and thanks to LIGO and NSF for their support.